Optical/Near–Infrared Observations of GRO J1744-28

D. M. Cole, D. E. Vanden Berk, S. A. Severson, M. C. Miller[1], J. M. Quashnock[1], R. C. Nichol, D. Q. Lamb

Department of Astronomy and Astrophysics

University of Chicago, Chicago, IL 60637

K. Hurley

Space Sciences Laboratory,

University of California, Berkeley, CA 94720-7450

P. Blanco

Center for Astrophysics and Space Studies

University of California, San Diego

La Jolla, CA 92093

C. Lidman

European Southern Observatory

Santiago, Chile

and

K. Glazebrook

Anglo-Australian Observatory

PO Box 296, Epping, NSW 2121, Australia

Received ______________________; accepted ______________________

---

[1] *Compton* Gamma-Ray Observatory Fellow

ABSTRACT

We present results from a series of optical (g and r-band) and near–infrared (K′-band) observations of the region of the sky including the entire XTE and ROSAT error circles for the "Bursting Pulsar" GRO J1744-28. These data were taken with the Astrophysical Research Consortium's 3.5-m telescope at Apache Point Observatory and with the 2.2-m telescope at the European Southern Observatory. We see no new object, nor any significant brightening of any known object, in these error circles, with the exception of an object detected in our 8 February 1996 image. This object has already been proposed as a near–infrared counterpart to GRO J1744-28. While it is seen in only two of our ten 8 February frames, there is no evidence that this is an instrumental artifact, suggesting the possibility of near–infrared flares from GRO J1744-28, similar to those that have been reported from the Rapid Burster. The distance to the "Bursting Pulsar" must be more than 2 kpc, and we suggest that it is more than 7 kpc.

Subject headings: Accretion, accretion disks — binaries: general — infrared: stars — stars: neutron

1. Introduction

On December 2, 1995, a new source of X-ray bursts lying in the direction of the galactic center was discovered using the Burst and Transient Source Experiment (BATSE) aboard the Compton Gamma-Ray Observatory (Fishman et al. 1995; Kouveliotou et al. 1996b). This source, GRO J1744-28, was an unusually frequent burster, with a maximum rate of 18 per hour on December 2 (Kouveliotou et al. 1996b) and an estimated rate of 40 per day at its brightest (Giles et al. 1996a). Subsequent BATSE observations showed that GRO J1744-28 is also a persistent emitter of X-rays (Paciesas et al. 1996), and found pulsations at 2.1 Hz both in the persistent emission (Finger et al. 1996a) and in the bursts (Kouveliotou et al. 1996a), making GRO J1744-28 the only known source of both periodic X-ray pulsations and frequent X-ray bursts and resulting in it being called the "Bursting Pulsar". Timing of the 2.1 Hz oscillations in the persistent X-ray emission revealed regular phase shifts with a period of 11.83 days, which have been interpreted as orbital motion in a binary (Finger, Wilson, & van Paradijs 1996). The low inferred mass function ($f_x(M) = 1.36 \times 10^{-4}\,M_\odot$, Finger et al. 1996b) and eccentricity ($e < 1.1 \times 10^{-3}$, Finger et al. 1996b) suggest that the neutron star in GRO J1744-28 is being fed by Roche lobe overflow from a low-mass red giant (Daumerie et al. 1996; Lamb, Miller, & Taam 1996; Sturner & Dermer 1996; Bildsten & Brown 1996; Joss & Rappaport 1996).

The optical brightness of many low-mass X-ray binaries (LMXBs) is thought to be dominated by reprocessing, in the accretion disk, of X-rays emitted from the surface of the neutron star. The counterpart to a transient LMXB is thus often identified by the detection of simultaneous brightening in other wavelengths (van Paradijs & McClintock 1994, 1995). Application of the empirical formulae of van Paradijs & McClintock (1994, 1995) indicates that if GRO J1744-28 is at the galactic center, the apparent unreddened visual magnitude due to reprocessing is approximately 12.5. An extension of the van Paradijs &

McClintock fits to the infrared suggests that at 8 kpc the unreddened K′ magnitude would be approximately 14 (Lamb, Miller, & Taam 1996), making GRO J1744-28 a good candidate for optical or infrared identification. Unfortunately, GRO J1744-28 was discovered when nearing closest approach to the Sun, making it temporarily impossible for any ground or space-based optical or infrared observatories to view it. Other transient LMXBs have active lifetimes of only a few months; the expected early demise of GRO J1744-28, coupled with its unique nature, led us to undertake an extensive series of observations in the optical and near-infrared during January and February, 1996, in hopes of finding a counterpart while it was possible.

Here we report our optical and infrared observations of GRO J1744-28. In § 2 we list the instruments and modes of operation we used during the search, and present our results for the infrared and optical variability in the entire Rossi X-ray Timing Explorer (RXTE) and ROSAT error boxes. In § 3 we discuss these results in light of models for the binary system in GRO J1744-28 and models for X-ray reprocessing, and place lower limits on the distance to GRO J1744-28. We also consider the near–infrared counterpart proposed by Augusteijn et al. (1996a); we show there is no reason to believe this object is an artifact, and that if it is associated with GRO J1744-28, the "Bursting Pulsar" exhibits flaring behavior similar to that of the Rapid Burster. Finally, in § 4 we give our conclusions.

2. Observations

2.1. Observational Procedure

Optical observations were made with the ARC 3.5-m telescope at Apache Point Observatory in New Mexico, using the Double Imaging Spectrograph (DIS). Via a dichroic (split at 5350 Å), this camera can observe simultaneously in both blue and red, through

Gunn g and r filters. The blue chip is a 512x512 SITe CCD and the red chip an 800x800 TI array, with pixel scales of $1\farcs1$ (blue) and $0\farcs61$ (red); the usable areas of the resulting images are approximately $6\farcm5$ x $4\farcm5$ (blue) and $5'$ x $4\farcm5$ (red).

Near–infrared observations were made with both the ARC and the European Southern Observatory's 2.2-m telescope. On the ARC, we used the Near Infrared Grism Spectrometer and Imager II (GRIM II), a 256 x 256 NICMOS array, with a Mauna Kea K' broadband filter (bandpass 1.95–2.30 μm). At f/5, the pixel scale is $0\farcs47$ and results in a $2'$ x $2'$ field of view. The skies were bright enough in the infrared throughout our search that we were forced to use neutral density (ND) filters. For most of our observations we used a 3% transmission filter, but in March we switched to a 25% one.

On the ESO 2.2-m, we used the IRAC2 camera, which is also a 256 x 256 NICMOS array, again with a Mauna Kea K' broadband filter. Images were taken using pixel scales of both $0\farcs278$ and $0\farcs507$, giving fields of view of about $1'$ and $2'$ on a side, respectively.

When we began observing GRO J1744-28 on 12 January 1996, it did not rise until after astronomical twilight had begun, and was only 25° from the Sun. The minimum elevation of the ARC 3.5-m is 6°; by the time GRO J1744-28 was high enough to be observed, the Sun was less than 10° below the horizon. This meant that the sky was already too bright to observe anywhere but in the near–infrared, and there were only 45 minutes until sunrise. Each day thereafter, however, the time between sunrise and when GRO J1744-28 became visible grew by nearly 4 minutes, and the sky at acquisition became darker; thus, by the beginning of February we were able to take relatively deep optical images in addition to the infrared.

2.2. Observational Log

We summarize our observations in Table 1. Our first observations were taken on the morning of 12 January 1996, when the best position we had for GRO J1744-28 was a parallelogram synthesized from Ulysses/GRB and GRO/BATSE observations measuring roughly $24'$ by $7'$ (Hurley et al. 1996). The central $10'$ by $6'$ portion of this parallelogram was covered with a 14-tile mosaic in K'; unfortunately, the eventual ROSAT position proved to be just off the edge of the easternmost tile.

We next observed on the morning of 21 January, by which date GRO J1744-28 was visible for a few minutes before the beginning of astronomical twilight. Its position had also been refined by observations made with the Rossi X-ray Timing Explorer (RXTE) to a circle approximately $2'$ in radius (Swank 1996). We were only able to cover about 25% of this error circle, with a mosaic of 2 tiles. Each tile is composed of two 5-second integrations through a 3% ND filter, giving the mosaic a 3-σ detection limit of magnitude 14.4 (Fig. 1a).

On 24 January we observed in the optical for the first time, generating g and r-band stacks of 28 and 37 seconds, respectively. The r-band image covers the entire RXTE error circle, and the g-band image the northern three-quarters; both cover the ROSAT position discussed below. The images have 3-σ detection limits of 15.5 (g) and 17.0 (r).

Our next observations were on 30 January. By that date, the RXTE position for GRO J1744-28 had shrunk to a circle approximately $1'$ in radius (Strohmayer, Jahoda, & Marshall 1996), meaning that the entire error circle lay within a single GRIM II field of view. Thus, rather than having to map out the error circle, we were able to simply stare at the region and try to catch the source in a burst. Ten-second K' images (still through a 3% ND filter) were taken every 15 seconds for over 30 minutes, from 12:42 to 13:13 UT; the telescope was dithered by $20''$ every five frames. An X-ray burst was recorded by Ulysses/GRB at 13:08:38, but did not coincide with any one image. Our previous frame

ended at 13:06:37, the next began at 13:09:01, and neither contained any flare.

The seeing was extremely variable during the 30 January observations. In fact, we could use only 53 of the 100 frames to construct a stacked image. However, these 53 frames give us an image equivalent to a 530-second integration with a 3-σ detection limit of magnitude 15.2 (Fig. 1b).

To complement the K′ data, we took more optical images of the field on 5 February. By then, the separation of GRO J1744-28 and the Sun was sufficient that we were able to take 15-second exposures for a period of about 90 minutes, dithering by about $20''$ between three positions. We constructed stacked images in g and r of 665 seconds each (Fig. 2), with 3-σ detection limits of magnitudes 20.5 and 19.7, respectively.

We made our first southern hemisphere observations on 8 February. Using the ESO 2.2-m, we took ten 60-second K′ frames, each dithered by $20''$. The stacked image has a 3-σ detection limit of 16.75 (Fig. 3). Due to the southern location of ESO, the airmass was much less than in the observations from Apache Point. The seeing in our ESO data is therefore much better ($\sim 0\overset{''}{.}6$), and the limiting magnitude is significantly improved.

Our work in January and February was predicated on the idea that like many transient LMXBs, the "Bursting Pulsar" would quickly fade from view, and therefore an immediate counterpart search was essential. By the end of February, though, GRO J1744-28 was well separated from the Sun and still strongly emitting and bursting in X-rays, and the field containing GRO J1744-28 was being routinely observed in many wavelengths. Still, it seemed likely that after three months, GRO J1744-28 would soon decline; therefore, on 3 March we observed again with the ARC 3.5-m to create one last K′ image. The sky by then was dark enough for us to use a 25% ND filter instead of the 3% filter, speeding things up considerably. Our stack of 54 5-second frames produced an image with a 3-σ detection limit of magnitude 16.3 (Fig. 4a).

In early March, GRO J1744-28 became sufficiently separated from the Sun for ASCA and ROSAT to observe it. The ASCA observations returned a position, good to $1'$, which partially overlaps the RXTE error circle, but is shifted by more than $1\farcm5$ to the northwest (Dotani et al. 1996). Shortly thereafter, ROSAT determined a position good to $8''$, consistent with the ASCA position and just outside the RXTE error circle (Kouveliotou et al. 1996c).[2] Most of our observations were based on the RXTE positions, and while they repeatedly cover its entire $1'$ radius error circle, the shift to the ROSAT position is enough to move GRO J1744-28 off the edge of many of our K′ frames due to the small fields of view of both the GRIM II and IRAC2 cameras. Still, the ROSAT error circle is covered by at least some K′ frames on every night we observed, as well as by all of our optical observations.

Although the "Bursting Pulsar" was active longer than we expected, the persistent emission from GRO J1744-28 declined continuously from January to March. In April, GRO J1744-28 was predicted to be undetectable by early May (Giles 1996);[3] indeed, it ceased being observable by GRO/BATSE on 3 May (Kouveliotou et al. 1996d). We therefore arranged to observe again with the ESO 2.2-m in order to obtain a deep baseline infrared image. We took 36 30-second K′ frames on 2 May, giving us an image with a 3-σ detection limit of 17.1, and an expanded plate scale of $0\farcs278$/pixel (Fig. 4b).

---

[2]At the 1996 HEAD meeting, J. Greiner of the ROSAT team (MPE Garching) indicated that the inclusion of systematic errors boosts the error radius to $10''$.

[3]In fact, RXTE was still detecting GRO J1744-28, as of August 30, 1996.

2.3. Results

To investigate the existence of any new or brightened objects in the optical in the error circles for GRO J1744-28, we visually compared our images with Palomar Sky Survey prints and ESO copies of UK Schmidt plates. We also overlaid our images with the digitized COSMOS/NRL source list, concentrating on the area within $2\farcm5$ of the RXTE position. In the infrared, we began by blink-comparing our observations with a 1992 NOAO set of J, H, and K images kindly provided by Mike Merrill (Merrill & Gatley, private communication). The 3-σ detection limit of this K image is about 14, at least a magnitude brighter than the images we took after 30 January. Therefore, we also blink-compared each of our infrared images with our deepest image (taken on 2 May), concentrating on the ROSAT error circle. These comparisons are summarized in Table 2.

We find no new objects nor any objects which have brightened by more than 0.5 magnitude in any optical observation. In the infrared, no objects differ from either the 1992 NOAO K-band image or our 2 May image, with one exception: our 8 February image contains an object, proposed as the near–infrared counterpart to GRO J1744-28 by Augusteijn et al. (1996a) through their comparison with their own March 28 K′ data (but see Augusteijn, Lidman, & Blanco 1996b and § 3). Using STScI Digitized Sky Survey scans and the IRAF/STSDAS GASP package, we find the position of this object to be $17^{\rm h}44^{\rm m}33\fs05 \pm 0\fs02$, $-28^\circ44'18\farcs6 \pm 0\farcs1$, placing it just on the edge of the ROSAT error circle. We also find the K′ magnitude of the object to be 15.7 ± 0.3, in agreement with that originally reported (Augusteijn et al. 1996a).

3. Discussion

3.1. Distance constraints

By combining our observations with models for GRO J1744-28, we can place limits on the distance to GRO J1744-28 and predict the K′ magnitude at which it must be seen (see Lamb, Miller, & Taam 1996 for details). The companion in GRO J1744-28 is believed to be a low-mass giant that is transferring material onto the neutron star via Roche lobe overflow (Daumerie et al. 1996; Lamb, Miller, & Taam 1996; Sturner & Dermer 1996; Bildsten & Brown 1996; Joss & Rappaport 1996). The intrinsic luminosity and effective temperature of the companion are then expected to be $20 - 30\,L_{\odot}$ and $T \approx 4300$ K (se, e.g., Lamb, Miller, & Taam 1996). The brightest near–infrared source in the ROSAT error box has K′=11 and there are no optical sources brighter than r=19.7. Given the expected luminosity and temperature of the companion, the lower distance limits (assuming $A_V \approx 3$ mag kpc^{-1} and $A_{K'} \approx A_V/9$ (Mathis 1990; Draine 1993)) are 1.5 kpc from the infrared limit and 2 kpc from the optical limit.

Another, somewhat more uncertain, limit may be derived by using the van Paradijs & McClintock (1994, 1995) relation between the X-ray luminosity and optical luminosity of low-mass X-ray binaries. For GRO J1744-28 their relation gives an absolute visual magnitude of $M_V \approx -2$. Again assuming a reddening of $A_V \approx 3$ mag kpc^{-1} and $A_{K'} \approx A_V/9$, our limit that no source had brightened at r=19.5 or brighter means that the distance to GRO J1744-28 must be greater than 3 kpc. An extension of the van Paradijs & McClintock relation to the infrared (Lamb, Miller, & Taam 1996), combined with our limit of $m_{K'} = 14$ for infrared brightening, gives a lower limit to the distance of 5 kpc. An entirely independent distance limit consistent with our lower limit was derived by Daumerie et al. (1996), who used the standard theory of disk accretion onto magnetized stars (Ghosh & Lamb 1979) to estimate the peak luminosity of GRO J1744-28. Combined with the peak observed flux, this model gives a distance greater than ~ 7 kpc. A distance of $\sim$8 kpc is

also supported by the angular proximity of GRO J1744-28 to the galactic center (only $20'$ away) and by the high neutral column density inferred from ASCA observations (Dotani et al. 1996). There is thus strong evidence that GRO J1744-28 is near the galactic center.

3.2. A Counterpart?

The object proposed by Augusteijn et al. (1996a) as the near–infrared counterpart to GRO J1744-28 is seen only in our 8 February image; we refer to it as the infrared candidate (IRC). The 8 February image is a stack of ten 60-second K' frames, each frame dithered by $\sim 10''$ to facilitate flatfielding. To further investigate the IRC, we examined the frames individually (Table 3 and Fig. 5). Of the ten frames, three were dithered such that the location of the IRC is off the edge of the array, and of the remaining seven frames, the IRC is seen in only two; this raises the possibility that the IRC is actually an artifact (Augusteijn, Lidman, & Blanco 1996b).

The IRAC2 NICMOS chip has defects, seen in the flatfield, which cause stars to fluctuate artificially. The IRC does not, however, coincide with any such defect in any frame. Moreover, a chip defect must move relative to the sky as the telescope is dithered—such an artifact can be seen in frames 8 and 9 of Figure 5—yet in these two frames the IRC is seen at the same position relative to nearby stars, although the frames were dithered by more than $20''$ (40 pixels).

The seven frames in which the IRC could have been seen have 3-σ detection limits of magnitude 15.5–15.6. With magnitude 14.6$\pm$0.4 in frame 4 and 15.0$\pm$0.4 in frame 8, the IRC is well above the detection limit; it is brighter, in fact, than two neighboring stars. In Figure 6 we compare the radial profile of the IRC (summed over both frames) with a point spread function constructed from the images of 10 stars of medium brightness. The two are

identical, within statistical noise; the IRC is not a single-pixel event.

If we examine the frames in the order in which they were taken, we see that the two frames in which the IRC is seen bracket the three in which it could not possibly have been seen (see Fig. 5). Thus, the two frames are neither isolated single frames nor contiguous. The detection of the IRC in those two frames is consistent either with an event covering 5 frames, and lasting at most 6 minutes, or with two or more events of average duration less than 3 minutes.

No X-ray bursts were recorded by Ulysses/GRB during the entire period of integration (09:26−09:42 February 8 UT), so if the IRC is an infrared burst or group of bursts from the companion to GRO J1744-28, the bursts are not correlated with X-ray bursts. We note, however, that infrared flares a few minutes apart, uncorrelated with X-ray bursts, have been reported from the Rapid Burster (Apparao et al. 1979; Kulkarni et al. 1979; Jones et al. 1980). The flares from the Rapid Burster are separated by between 50 and 150 seconds, with total energies (assuming isotropic emission and a distance of 10 kpc) of between $\sim 6 \times 10^{37}$ ergs and $\sim 3 \times 10^{38}$ ergs.

We conclude that there is no convincing instrumental reason to doubt the reality of the images seen on these two 8 February frames, and no obvious astrophysical reason that such images could not be related to GRO J1744-28. Figure 7 shows the light curve for the IRC over the entire period of our observations (21 January – 2 May 1996) and (see inset) during the 8 February 1996 exposure. Further observations are necessary; in particular, if the IRC is the counterpart, a persistent source at this location is expected with $m_{K'} < 20$ (Lamb, Miller, & Taam 1996).

If the IRC is an infrared burst or group of bursts from GRO J1744-28, the minimum total energy in the bursts may be estimated by comparing this with the 2 May image, in which the companion must be fainter than $m_{K'} \approx 17.1$. Assuming isotropic emission and

using a companion luminosity of 20 $L_\odot$, the average luminosity of the flare in the two frames in which it was detected was at least $L \approx 250\, L_\odot$. If the flares only occurred in two one-minute frames, this implies a total energy of $\sim 10^{38}$ ergs, similar to that seen from the Rapid Burster. This is a minimum, because in principle the source could have been arbitrarily bright in the three intervening frames, where the candidate was out of the field of view.

In addition, if the IRC is the counterpart, we can place two more lower limits on to the distance to GRO J1744-28. In our 2 May image, nothing is seen at the location of the IRC to $m_{K'} = 17.1$; combined with the luminosity estimates for the companion, this implies a distance of more than 7 kpc. Similarly, if the IRC is the counterpart, the fact that no sources were seen at the location of the IRC to $m_{K'} = 15.5$ in five 8 February frames implies a distance of ~7 kpc. The main uncertainty in both estimates is the amount of reddening to the galactic center, which could be between $A_{K'} = 2$ and $A_{K'} = 4$ (Mathis 1990).

4. Conclusions

We observed the region of the sky including the entire RXTE and ROSAT error circles for GRO J1477-28 multiple times in both the infrared (K′-band) and in the optical (g and r-bands). These observations allow allow us to put strict lower limits on the distance to GRO J1744-28 of 1.5 kpc (infrared) and 2 kpc (optical), or, depending on the X-ray reprocessing model chosen, 5 kpc (infrared) and 3 kpc (optical). Our 8 February observations show a possible near–infrared counterpart to the “Bursting Pulsar” at $17^{\mathrm{h}}44^{\mathrm{m}}33\overset{\mathrm{s}}{.}05 \pm 0\overset{\mathrm{s}}{.}02$, $-28^\circ 44' 18\overset{''}{.}6 \pm 0\overset{''}{.}1$; if this is indeed the counterpart, we can place a further limit on the distance to GRO J1744-28 of more than 7 kpc. Additional observations are needed; in particular, a near–infrared image of this field which reaches a limiting magnitude of K′=20.

We must acknowledge the extraordinary efforts made by the observing specialists at APO, without whom this project would have been impossible: E. Bergeron, K. Gloria, and D. Long. DMC wishes to thank his advisor, D. A. Harper, for allowing him to embark on this diversion from his thesis. The authors also wish to acknowledge the following sources of support: NASA Space Telescope Grant GO-06007.01-94 (DEVB), Compton GRO fellowships NAGW 5-2687 (MCM) and NAGW 5-2660 (JMQ), NASA grant NAG 5-2868 (DQL), and JPL Contract 958056 for the Ulysses/GRB experiment (KH).

REFERENCES

Augusteijn, T., van Paradijs, J., Kouveliotou, C., Greiner, J., Fishman, G. J., Rutledge R., and Lewin W. H. G. 1996a, IAU Circ., No. 6369

Augusteijn, T., Lidman, C., and Blanco, P. 1996b, IAU Circ., No. 6484

Bildsten, L., and Brown, E. F. 1996, ApJ, submitted

Daumerie, P., Kalogera, V., Lamb, F. K., and Psaltis, D. 1996, Nature, 382, 141

Dotani, T., Ueda, Y., Nagase, F., Inoue, H., and Kouveliotou, C. 1996, IAU Circ., No. 6368

Draine, B. T. 1993, in *The First Symposium on the Infrared Cirrus and Diffuse Interstellar Clouds*, eds R. Cutri and W. Latter, ASP Conf. Series, in press.

Finger, M. H., Wilson, R. B., Harmon, B. A., Hagedon, K., and Prince, T. A. 1996a, IAU Circ., No. 6285

Finger, M. H., Wilson, R. B., and van Paradijs, J. 1996, IAU Circ., No. 6286

Finger, M. H., Koh, D. T., Nelson, R. W., Prince, T. A., Vaughan, B. A., and Wilson, R. B. 1996b, Nature, 381, 291

Fishman, G. J., Kouveliotou, C., van Paradijs, J., Harmon, B. A., Paciesas, W. S., Briggs, M. S., Kommers, J., and Lewin, W. H. G. 1995, IAU Circ., No. 6272

Ghosh, P., and Lamb, F. K. 1979, ApJ, 234, 296

Giles, A. B. 1996, IAU Circ., No. 6385

Giles, A. B., Swank, J. H., Jahoda, K., Zhang, W., Strohmayer, T. E., Stark, M. J., and Morgan, E. H. 1996, ApJ, 469, L25

Hurley, K., Kouveliotou, C., Harmon, A., Fishman, G. J., Briggs, M., van Paradijs, J., Kommers, J., and Lewin, W. H. G. 1996, IAU Circ., No. 6286

Joss, P. C., and Rappaport, S. 1996, Science, submitted

Kouveliotou, C., Kommers, J., Lewin, W. H. G., van Paradijs, J., Fishman, G. J. and Briggs, M. 1996a, IAU Circ., No. 6286

Kouveliotou, C., van Paradijs, J., Fishman, G. J., Briggs, M. S., Kommers, J. M., Harmon, B. A., Meegan, C. A., and Lewin, W. H. G. 1996b, Nature, 379, 399

Kouveliotou, C., Greiner, J., van Paradijs, J., Fishman, G. J., Lewin, W. H. G., Rutledge, R., Kommers, J., and Briggs, M. S. 1996c, IAU Circ., No. 6369

Kouveliotou, C., Deal, K., Woods, P., Briggs, M., Harmon, B. A., Fishman, G. J., van Paradijs, J., Finger, M. H., Kommers, J., and Lewin, W. H. G. 1996d, IAU Circ., No. 6395

Lamb, D. Q., Miller, M. C., and Taam, R. 1996, in preparation

Mathis, J. 1990 ARA&A, 28, 37

Paciesas, W. S., Harmon, B. A., Fishman, G. J., Zhang, S. N., and Robinson, C. R. 1996, IAU Circ., No. 6284

Strohmayer, T., Jahoda, K., and Marshall, F. 1996, IAU Circ., No. 6309

Sturner, S. J., and Dermer, C. D. 1996, ApJ, 465, L31

Swank, J. 1996, IAU Circ., No. 6291

van Paradijs, J., and McClintock, J. E. 1994, A&A, 290, 133

van Paradijs, J., and McClintock, J. E. 1995, in X-Ray Binaries, eds. Lewin, W. H. G., van Paradijs, J., and van den Heuvel, E. P. J., pg. 58

Table 1. Observations.

Date	UT	Passband	Exposure (sec)	Area Covered
24 Jan	13:06−13:16	g	28	$17^{h}44^{m}22\overset{s}{.}0 - 51\overset{s}{.}8$, $-28°41'00'' - 45'38''$
		r	37	$17^{h}44^{m}19\overset{s}{.}7 - 54\overset{s}{.}2$, $-28°41'14'' - 46'19''$
5 Feb	11:47−12:58	g	665	$17^{h}44^{m}17\overset{s}{.}2 - 43\overset{s}{.}0$, $-28°42'38'' - 46'57''$
		r	665	$17^{h}44^{m}21\overset{s}{.}2 - 40\overset{s}{.}1$, $-28°42'52'' - 46'51''$
12 Jan	13:25−13:36	K′	10	$17^{h}43^{m}45^{s} - 44^{m}33^{s}$, $-28°42'00'' - 48'24''$
21 Jan	13:36−13:39	K′	10	$17^{h}44^{m}29\overset{s}{.}1 - 38\overset{s}{.}2$, $-28°44'07'' - 47'42''$
30 Jan	12:42−13:13	K′	530	$17^{h}44^{m}29\overset{s}{.}1 - 38\overset{s}{.}2$, $-28°44'05'' - 46'04''$
8 Feb	09:26−09:38	K′	600	$17^{h}44^{m}28\overset{s}{.}0 - 39\overset{s}{.}5$, $-28°44'08'' - 46'38''$
3 Mar	12:37−12:47	K′	270	$17^{h}44^{m}32\overset{s}{.}8 - 37\overset{s}{.}2$, $-28°44'13'' - 45'37''$
2 May	07:43−08:16	K′	1080	$17^{h}44^{m}29\overset{s}{.}3 - 37\overset{s}{.}4$, $-28°43'33'' - 45'03''$

Note. — The 8 February and 2 May observations were done at ESO; all the rest at APO.

Table 2. Image Comparisons

Date	Passband	Region of Comparison	Area $\square'$	Magnitude Limit	Notes
24 Jan	g	$17^{h}44^{m}22.^{s}9 - 45.^{s}7$, $-28^{\circ}42'52'' - 45'38''$	11.15	15.5 ± 0.5	a
	r	$17^{h}44^{m}22.^{s}9 - 45.^{s}7$, $-28^{\circ}42'52'' - 46'19''$	14.63	17.0 ± 0.5	b
5 Feb	g	$17^{h}44^{m}22.^{s}9 - 43.^{s}0$, $-28^{\circ}42'52'' - 46'57''$	18.49	20.5 ± 0.3	a
	r	$17^{h}44^{m}22.^{s}9 - 40.^{s}1$, $-28^{\circ}42'52'' - 46'51''$	13.31	19.7 ± 0.3	b
21 Jan	K'	$17^{h}44^{m}28.^{s}8 - 37.^{s}4$, $-28^{\circ}44'10'' - 47'45''$	6.75	$\sim$14	c
	K'	$17^{h}44^{m}31.^{s}0 - 35.^{s}6$, $-28^{\circ}44'07'' - 45'03''$	0.94	14.4 ± 0.3	d
30 Jan	K'	$17^{h}44^{m}29.^{s}1 - 38.^{s}0$, $-28^{\circ}44'10'' - 46'10''$	3.90	$\sim$14	c
	K'	$17^{h}44^{m}30.^{s}9 - 35.^{s}6$, $-28^{\circ}44'05'' - 45'11''$	1.13	15.2 ± 0.3	d
8 Feb	K'	$17^{h}44^{m}32.^{s}0 - 34.^{s}3$, $-28^{\circ}44'10'' - 44'45''$	0.29	$\sim$14	c
	K'	$17^{h}44^{m}30.^{s}8 - 35.^{s}6$, $-28^{\circ}44'08'' - 45'08''$	1.05	16.75 ± 0.3	d
3 Mar	K'	$17^{h}44^{m}32.^{s}8 - 34.^{s}3$, $-28^{\circ}44'10'' - 44'45''$	0.19	$\sim$14	c
	K'	$17^{h}44^{m}32.^{s}8 - 34.^{s}3$, $-28^{\circ}44'08'' - 44'45''$	0.20	16.3 ± 0.3	d

[a] Compared with a POSS print and the COSMOS/NRL list.

[b] Compared with an ESO copy of a UK Schmidt plate and the COSMOS/NRL list.

[c] Compared with a 1992 NOAO K image, limiting magnitude approximately 14.

[d] Compared with the 2 May observation, limiting magnitude 17.1 ± 0.3.

Note. — The second RXTE error circle is $17^{h}44^{m}34.^{s}3 \pm 2.^{s}8$, $-28^{\circ}45'22'' \pm 47''$ (Strohmayer, Jahoda, & Marshall 1996), while the ROSAT error circle is $17^{h}44^{m}33.^{s}1$, $-28^{\circ}44'29''$, both $\pm 10''$ (Kouveliotou et al. 1996c). The region of comparison for any optical observation is really that portion of a $2'.5$ radius circle centered on the second RXTE position–the extent of our COSMOS/NRL list–which overlaps the image.

Table 3. 8 February 1996 Frames.

Frame Number	UT	Candidate Seen	Limiting Magnitude	X & Y Shifts (pixels)
1	09:27–09:28	No	15.5	18.7, 0.4
2	09:28–09:29	No	15.5	19.2, 20.1
3	09:30–09:31	No	15.6	0.4, 20.0
4	09:31–09:32	Yes	15.5	0.0, 0.0
5	09:33–09:34	off top	-	2.0, -19.5
6	09:35–09:36	off top	-	23.3, -19.9
7	09:37–09:38	off top	-	42.9, -19.8
8	09:38–09:39	Yes	15.6	43.2, -0.8
9	09:40–09:41	No	15.5	41.8, 18.6
10	09:41–09:42	No	15.5	21.8, 0.2

Note. — The magnitudes of the IRC in frames 4 and 8 are 14.6 ± 0.4 and 15.0 ± 0.4, respectively.

Fig. 1.— K′, 21 January 1996 (a) and 30 January 1996 (b), APO. The ROSAT error circle is marked.

Fig. 2.— g-band (a) and r-band (b), 5 February 1996, APO. The ROSAT error circle is marked.

Fig. 3.— K′, 8 February 1996, ESO. The IRC is visible at the top of the ROSAT error circle (see also Fig. 5).

Fig. 4.— K′, 3 March 1996, APO (a) and 2 May 1996, ESO (b). The ROSAT error circle is marked.

Fig. 5.— Montage of the frames taken on 8 February. The sequence begins in the lower left corner, runs up the left column, then up the right column. The white arrows point to the IRC in frames 4 and 8. The location of the IRC is off the edge of frames 5–7. A chip artifact is visible in frames 8 and 9.

Fig. 6.— Radial profile of the IRC. The smooth curve shows the point spread function, obtained from 10 stars of medium brightness.

Fig. 7.— The light curve for the IRC over the entire period of our observations (21 January – 2 May 1996) and (see inset) during the 8 February 1996 exposure (see Tables 2 and 3). The open symbol is from Augusteijn et al. 1996a. The dashed limit is for the 8 February frames in which the IRC does not appear.

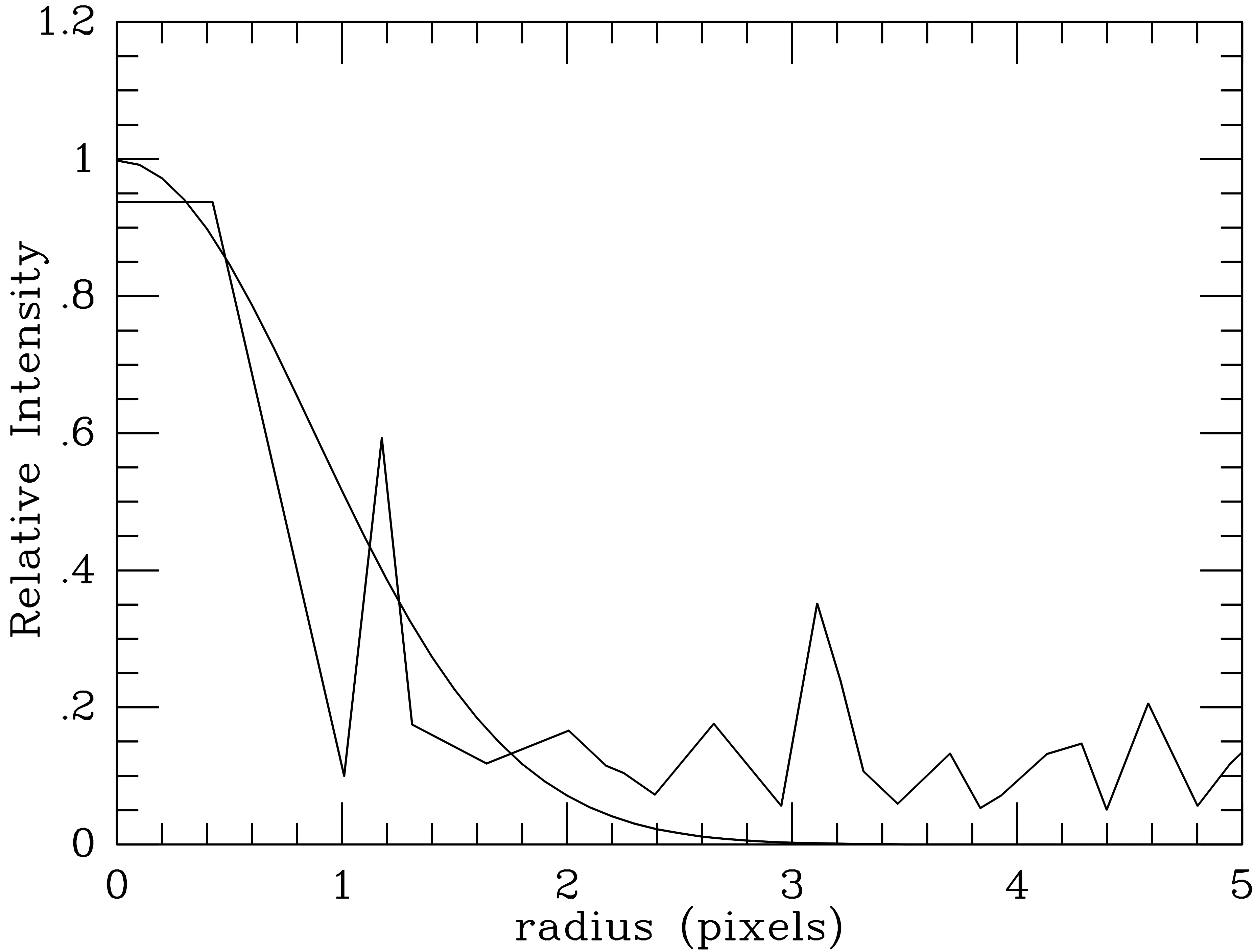

1.2
1
.8
.6
.4
.2
0
Relative Intensity
0
1
2
3
4
5
radius (pixels)

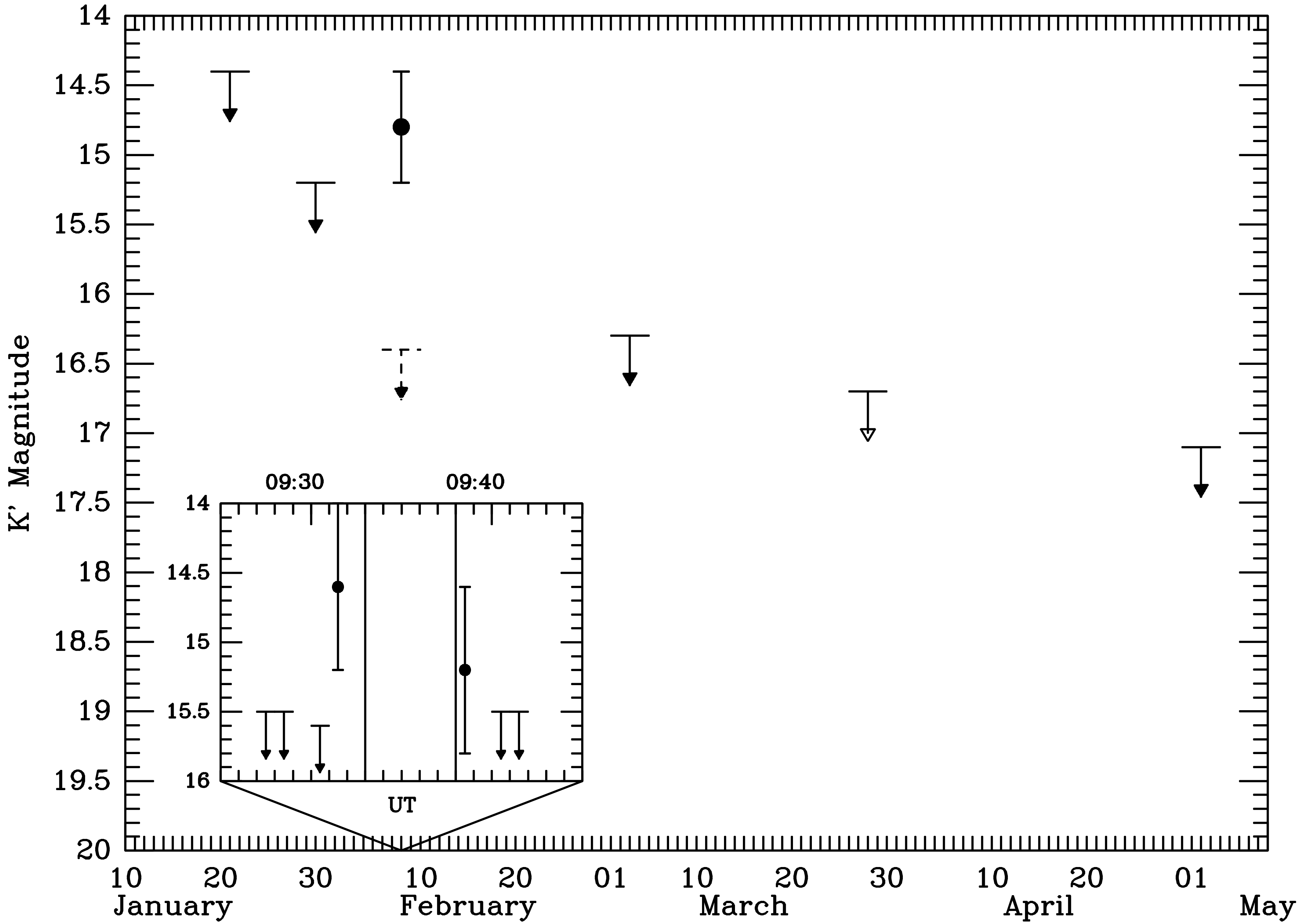
K' Magnitude
14
14.5
15
15.5
16
16.5
17
17.5
18
18.5
19
19.5
20
10
20
30
10
20
01
10
20
30
10
20
01
January
February
March
April
May
09:30
09:40
UT
14
14.5
15
15.5
16